land

MDPI

Article

Risk Assessment and Spatial Zoning of Rainstorm and Flood Hazards in Mountainous Cities Using the Random Forest Algorithm and the SCS Model

Zixin Xie [1] and Bo Shu [2,*]

[1] School of Architecture and Civil Engineering, Xihua University, Chengdu 611756, China; 212023095300012@stu.xhu.edu.cn
[2] School of Design, Southwest Jiaotong University, Chengdu 611756, China
* Correspondence: shubo@swjtu.edu.cn

Abstract: China has a vast land area, with mountains accounting for 1/3 of the country's land area. Flooding in these areas can cause significant damage to human life and property. Therefore, rainstorms and flood hazards in Huangshan City should be accurately assessed and effectively managed to improve urban resilience, promote green and low-carbon development, and ensure socio-economic stability. Through the Random Forest (RF) algorithm and the Soil Conservation Service (SCS) model, this study aimed to assess and demarcate rainstorm and flood hazard risks in Huangshan City. Specifically, Driving forces-Pressure-State-Impact-Response (DPSIR)'s framework was applied to examine the main influencing factors. Subsequently, the RF algorithm was employed to select 11 major indicators and establish a comprehensive risk assessment model integrating four factors: hazard, exposure, vulnerability, and adaptive capacity. Additionally, a flood hazard risk zoning map of Huangshan City was generated by combining the SCS model with a Geographic Information System (GIS)-based spatial analysis. The assessment results reveal significant spatial heterogeneity in rainstorm and flood risks, with higher risks concentrated in low-lying areas and urban fringes. In addition, precipitation during the flood season and economic losses were identified as key contributors to flood risk. Furthermore, flood risks in certain areas have intensified with ongoing urbanization. The evaluation model was validated by the 7 July 2020 flood event, suggesting that Huangshan District, Huizhou District, and northern Shexian County suffered the most severe economic losses. This confirms the reliability of the model. Finally, targeted flood disaster prevention and mitigation strategies were proposed for Huangshan City, particularly in the context of carbon neutrality and green urbanization, providing decision-making support for disaster prevention and emergency management. These recommendations will contribute to enhancing the city's disaster resilience and promoting sustainable urban development.

Keywords: flood hazard risk assessment; random forest algorithm; SCS model; risk spatial zoning; mountainous city

Academic Editor: Faccini Francesco

Received: 4 February 2025
Revised: 19 February 2025
Accepted: 20 February 2025
Published: 22 February 2025

Citation: Xie, Z.; Shu, B. Risk Assessment and Spatial Zoning of Rainstorm and Flood Hazards in Mountainous Cities Using the Random Forest Algorithm and the SCS Model. *Land* **2025**, *14*, 453. https://doi.org/10.3390/land14030453

1. Introduction

Flood-related catastrophes have become one of the global risks directly induced by the increasing scale of climate change and extreme climatic terms. Flood disasters have intensified regarding frequency and magnitude in recent decades, as revealed in global climate reports under the United Nations Framework Convention on Climate Change

(UNFCCC). This carries not only a high toll of lives and assets but also a strong impact on the environment, food production, and urban systems.

In China, flood disasters are increasing. Particularly, the southern regions are highly susceptible because of their complex terrain and concentrated precipitation, making rain-induced mountain floods and urban waterlogging common types of severe disasters [1]. Statistical data from the China Meteorological Administration and water resources authorities suggest that torrential rains and mountain floods in the south have significantly affected local socio-economic conditions and people's livelihoods in recent years. Huangshan City, a representative mountainous city in southern China, encounters particularly pronounced flood hazards. In this context, the Huangshan municipal government proposed the Huangshan Modern Water Network Construction Plan (2024) to strengthen its disaster prevention and mitigation capability [2].

The importance of integrating disaster prevention and ecological civilization development in the context of carbon neutrality has become more prominent as the goals of ecological civilization and carbon neutrality continue to be pursued. With the speedy development of the digital economy, big data analytics and intelligent technologies can be presumably applied for disaster risk assessment. In this way, Huangshan City can obtain more precise tools for rainfall forecasting and hydrological alteration detection, laying a science-based foundation for decision-making [3]. Thus, scientifically assessing the risk of rain and flood disasters in Huangshan City contributes to not only formulating more precise countermeasures to reduce disaster losses but also raising the public's awareness of disaster prevention and promoting green and sustainable development. Additionally, this process provides references for other parts of the world that face similar challenges and ultimately enhance disaster resilience and environmental sustainability globally.

Internationally, relatively comprehensive rainstorm and flood hazard risk assessment and disaster prevention systems have been established, particularly in countries such as the United States and Japan. Early studies primarily focused on response measures for individual disaster events and employed traditional hydrological models, such as the Hydrologic Engineering Center's Hydrologic Modeling System (HEC-HMS) and the Storm Water Management Model (SWMM), to simulate watershed flooding. By reconstructing rainfall-runoff processes, these models laid a scientific foundation for flood control design and emergency planning [4]. Risk assessment has expanded from analyzing individual disaster types to comprehensive multi-hazard evaluations with further research advancements [5]. For instance, Japan has integrated early warning systems with community-based disaster prevention networks, bringing about significantly reinforced public disaster awareness and response capabilities [6]. In the United States, national-level emergency management systems (such as the Federal Emergency Management Agency (FEMA)) and regional flood emergency response plans have been developed to strengthen disaster coordination before and after flood events [7]. Over the years, these research efforts eventually developed into comprehensive crisis management schemes for handling issues from pre-disaster risk assessment to emergency response during disasters to post-disaster recovery. Currently, flood hazard risk assessment has become a hot topic in worldwide research, with more and more findings [8–10]. In recent years, researchers have paid growing attention to the coupling relationship between floods induced by rainstorms and secondary disasters, including debris flows and landslides, as well as integrated spatiotemporal models for multi-hazard risk assessment. Flood hazard risk research is not new internationally and can be traced back to the 1950s. In 1991, the United Nations explicitly defined risk as "the expected impact of certain natural disasters or social events on human life safety and economic losses" [11,12]. Subsequently, researchers further refined this definition [13–15], establishing that flood hazards stem from the combined effects of hazard-inducing factors,

disaster-prone environments, and exposed elements [16]. This drove the development of a four-dimensional flood risk assessment framework, involving hazard-inducing factors, disaster-prone environments, exposed elements, and disaster prevention and mitigation measures [17]. In accordance with the differences in data sources, data processing techniques, and assessment methodologies, existing flood risk assessment approaches can be broadly categorized into four types: historical disaster data analysis, scenario-based dynamic simulation, indicator-based assessment methods, and integrated approaches combining GIS and remote sensing (RS) technologies.

Currently, advancements in machine learning have introduced new approaches to flood hazard risk assessment, and the RF algorithm has emerged as a particularly popular tool attributed to its adaptability and ability to process complex datasets [18]. Compared to traditional physical models, RF excels at handling intricate interactions among multiple influencing factors by constructing multiple decision trees to enhance predictive accuracy, rendering it specifically effective in complex terrains. For example, Chen et al. [19,20] designed an urban flood hazard assessment framework through the Driving-Pressure-State-Impact-Response (DPSIR) model for the Yangtze River Delta. Using the RF algorithm, they identified 15 key flood risk indicators (including impervious urban surfaces and precipitation levels during the flood season) and constructed a flood risk assessment model. Similarly, Anderson et al. [21] integrated machine learning with numerical simulations to assess coastal flood risks in San Diego, California, while evaluating potential impacts of future climate change. The advantages of the RF algorithm extend beyond its efficiency in data processing. Unlike traditional methods relying heavily on precise physical model assumptions and data inputs, RF can efficiently analyze large-scale, high-dimensional datasets. Wang et al. [22] adopted an RF-based assessment model to evaluate regional flood risks in the Dongjiang River Basin, China, selected 11 risk indicators, and generated 5000 samples for model training and testing. Additionally, Hao et al. [23] employed RF to predict potential terrorism risks in the Indochina Peninsula across a spatial scale involving 15 driving factors, demonstrating its versatility in hazard assessment. Moreover, RF offers intuitive rankings of variable importance and thus facilitates the identification of key flood risk factors. This capability enhances disaster prevention, emergency response, and policy formulation efforts [24–26], enabling RF to be a valuable tool in the field of flood risk assessment and management.

The Soil Conservation Service Curve Number (SCS-CN) method, a widely used empirical formula, has obtained increasing attention in recent years for its application in rainstorm and flood hazard risk assessment [27]. By incorporating factors such as precipitation, soil type, land use, land cover, and antecedent soil moisture, this method allows for rapid estimation of regional runoff and provides effective support for flood risk evaluation. For instance, Jia et al. [28] utilized a GIS-based SCS-CN approach to evaluate flood risks at cultural heritage sites in Shanxi Province under three different Shared Socioeconomic Pathway (SSP) climate change scenarios (SSP119, SSP245, and SSP585) projected to the end of the 21st century. By combining the Land Use Scenario Dynamics-Urban (LUSD-urban) model with the SCS-CN method, Fang et al. [29] proposed a novel approach for estimating future surface runoff through Urban Ecosystem Integrity (UEI) analysis. Additionally, Ei et al. [30] applied meteorological and morphological data analysis while merging the SCS Curve Number method for precipitation loss estimation with the SCS-Hydrograph for runoff transformation. Their model was implemented in two watersheds (An-Nawayah and Al-Rashrash) southeast of Cairo, Egypt. Compared to traditional hydrological models, the SCS-CN method presents notable advantages, consisting of operational simplicity, fast computation speed, and minimal data requirements for topographic and meteorological inputs. Thus, it is particularly suitable for regions with limited data availability or com-

putational resources. However, the method also possesses certain limitations, especially when it is applied to complex terrains or extreme climate events, where its accuracy and applicability may be constrained. To overcome these limitations, researchers have increasingly integrated the SCS-CN method with advanced technologies such as remote sensing (RS), Geographic Information Systems (GIS), and machine learning algorithms [31]. For example, Yin et al. [32,33] successfully enhanced risk assessment accuracy and efficiency by combining the RF algorithm with the SCS-CN method, revealing the significant potential of this integrated approach. Such methodological integrations can reinforce model robustness while enhancing its sensitivity to multiple variables, particularly in complex environmental conditions.

Nonetheless, there is insufficient current research on the integration of the RF algorithm with the Soil Conservation Service (SCS) model for assessing rainstorm and flood hazards in mountainous cities. Specifically, the RF algorithm has demonstrated clear advantages in handling complex datasets and capturing nonlinear relationships, contributing to its widespread application in precipitation forecasting and watershed hydrological modeling. However, its effective integration with the SCS model under the unique topographic conditions, complex hydrological processes, and multiple impacts of climate change in mountainous cities has yet to be fully explored. The SCS model is well-suited for simulating rainfall-runoff processes, especially at the watershed scale. However, the model faces notable limitations in capturing complex hydrological characteristics and spatial heterogeneity when being applied to mountainous urban environments. By leveraging the strengths of the RF algorithm, it can be integrated with the SCS model to compensate for the latter's shortcomings in dynamic prediction and adaptive adjustments, thereby improving the accuracy and reliability of flood risk assessment in complex mountainous urban settings. Overall, exploring this integrated approach holds significant academic value and practical application potential. It may also assist in more accurate flood hazard early warning, risk evaluation, and emergency management for mountainous cities, so as to facilitate urban sustainability and disaster resilience.

This study aimed to integrate the RF algorithm with the Soil Conservation Service Curve Number (SCS-CN) method and conduct a detailed assessment and zoning of flood hazards in Huangshan City by leveraging Geographic Information System (GIS) technology. The SCS-CN method, as a simple yet effective empirical formula, accounts for factors such as precipitation, soil type, and land use to rapidly estimate regional runoff, providing crucial support for flood risk evaluation. Meanwhile, the RF algorithm with the automatic selection of key flood risk factors can effectively handle complex spatial data and nonlinear relationships to enhance prediction accuracy. The two approaches may complement each other. In this study, they were integrated to optimize their individual strengths for obtaining reliable assessment results and achieving accurate identification of high-risk areas. The findings ultimately inform disaster prevention and mitigation strategies that are more tailored to the local context and support flood risk management in Huangshan City.

2. Study Area and Date Description

2.1. Study Area Description

Huangshan City is located in southern Anhui Province, at the transition zone between the middle and lower reaches of the Yangtze River Plain and the mountainous region [34]. It is located in longitudes from 117°30′ to 118°30′ E and latitudes from 29°24′ to 30°20′ N (Figure 1). Huangshan City administers Tunxi District, Huangshan District, Huizhou District, and several counties, and the world-renowned Huangshan Scenic Area was awarded the World Natural and Cultural Heritage by UNESCO. Huangshan has a complex topography, with mountainous and hilly plains, composed of several mountain ranges,

with Fanshu Mountain as its center. It is mainly granite upon which peculiar rock edifices and steep terrains form [35]. Huangshan City has a subtropical monsoon climate with four distinct seasons. Its annual average temperature and yearly average precipitation are around 16 °C and 1800–2400 mm, mainly during the plum rain and typhoon seasons.

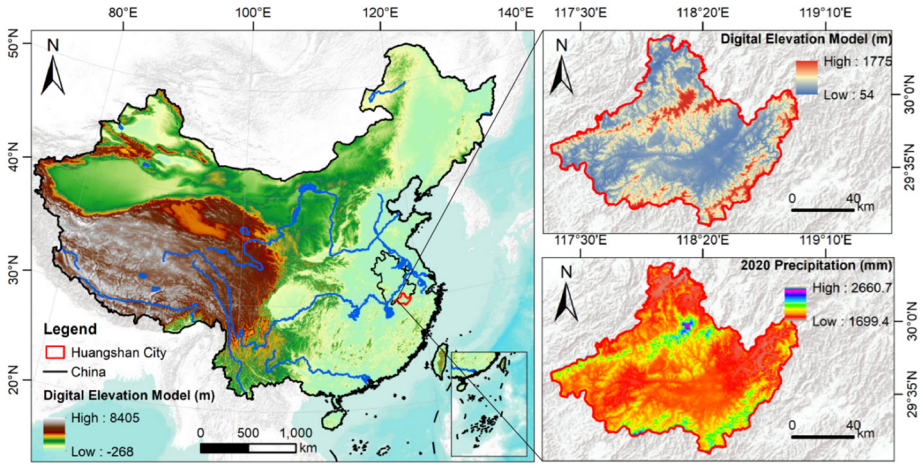

Figure 1. The regional schematic diagram of Mount Huangshan City.

The resident population in 2022 will be about 1.33 million, with an urbanization rate of 55%, but the mountainous areas are sparsely populated and vulnerable. The economy is highly dependent on tourism, with a monolithic structure that makes it less resilient to disasters. The problem of aging is prominent, with 22% of the population over 60 years old, a serious exodus of young adults, increasing rural "hollowing out", and insufficient disaster response capacity for the elderly and children left behind. Infrastructure is lagging behind, and the level of transportation, medical care, and other public services in remote mountainous areas is low, constraining the ability to prevent and mitigate disasters. The city of Huangshan needs to promote economic diversification and upgrade public services and disaster prevention capabilities to cope with natural disasters and socio-economic challenges while protecting the ecology.

Despite advances in flood hazard risk assessment for Huangshan City, research in this area is still scarce, and most of them emphasize single-hazard assessments. There is a long road to achieving a systematic and multi-layered comprehensive risk analysis. Thus, detailed research on flood hazard risks in Huangshan City, especially the combination of machine learning algorithms and hydrological models, has great academic and practical significance.

Huangshan City has a long history of frequent rainstorms and flood disasters. *The Huizhou Prefecture Chronicles* recorded multiple instances of mountain floods and debris flows triggered by heavy rainfall during the Ming and Qing dynasties. In recent years, extreme rainfall events and flooding have increased in frequency and severity because of climate change (Appendix A). In 1991, 2006, and 2011, there were major floods in Henan. Moreover, a significant flood exerted a substantial impact on a national examination called "Gaokao" in July 2020. Annual precipitation has continued to rise from my parent's time (10%), and extreme weather events have increased recently. Increasingly extreme rainfall has elevated the risks of floods and geological disasters. Flood risk assessment is performed on a strong foundation of historical meteorological and hydrological data. Integrating and embedding GIS technology into the SCS model play a supportive role in formulating effective disaster prevention and mitigation measures, contributing to the enhanced flood resilience in Huangshan City.

2.2. Date Description

This study needs to deal with the following types of data, which are pre-processed by technical means to ensure the accuracy and completeness of the data. According to the research factors to be selected for rain and flood risk assessment, the selected data sources and contents are shown in Table 1.

Table 1. Basic data and sources.

Data Type	Data Source	Data Content	Time Span
Topographic Data	National Geospatial Information Center (https://www.webmap.cn/main.do?method=index (accessed on 11 September 2024))	Digital Elevation Model (DEM) data (30 m resolution)	Long-term observation
Precipitation Data	National Meteorological Science Data Center (https://data.cma.cn/ (accessed on 11 September 2024))	Daily rainfall data	Last 50 years
Soil Data	FAO Soil Database (https://www.fao.org/soils-portal/en/ (accessed on 11 September 2024))	Soil type, permeability, moisture content	Long-term observation
Vegetation Data	Huangshan Ecology and Environment Bureau (https://sthjj.huangshan.gov.cn/ (accessed on 15 September 2024))	Vegetation type, coverage, density	Dynamic data
Transportation Data	National Geospatial Information Resource Directory Service System (https://www.webmap.cn/main.do?method=index (accessed on 11 September 2024))	Road network distribution	Real-time updates
Population Density	Huangshan Statistics Bureau (https://tjj.huangshan.gov.cn/ (accessed on 11 September 2024))	Population density distribution by region	10-year census data
Land Use Data	National Geospatial Information Resource Directory Service System (https://www.webmap.cn/main.do?method=index (accessed on 11 September 2024))	Land use types and spatial distribution	5 years
Economic Data	Huangshan Statistics Bureau (https://tjj.huangshan.gov.cn/ (accessed on 15 September 2024))	Economic development level, economic loss assessment, GDP per km^2	10-year economic census data
Urbanization Rate	Huangshan Statistics Bureau (https://tjj.huangshan.gov.cn/ (accessed on 15 September 2024))	Urbanization level by region	10-year statistical data
Per Capita Arable Land	Ministry of Agriculture and Rural Affairs (http://www.moa.gov.cn/ (accessed on 15 September 2024))	Per capita arable land in each county/district	Real-time updates
Built-up Area Road Network Density	National Geospatial Information Resource Directory Service System (https://www.webmap.cn/main.do?method=index (accessed on 11 September 2024))	Road network density per unit area of built-up land	Real-time updates
Municipal Flood Control Investment	Huangshan Water Resources Bureau (https://slj.huangshan.gov.cn/ (accessed on 15 September 2024))	Investment in flood control infrastructure per unit area	Real-time updates

Rainstorm and flood hazard risk assessment and zoning rely on the comprehensive processing and analysis of multi-source data. With Geographic Information System (GIS) technology and the Soil Conservation Service (SCS) model, in this study, the following categories of data are processed, and technical methods are applied for data preprocessing to ensure accuracy and completeness. The selected research factors and corresponding data sources for flood hazard risk assessment are summarized in Table 2 [36]. Additionally, data preprocessing is conducted by GIS technology and the SCS model to reinforce data quality and improve the reliability of risk assessment.

Table 2. Significance assessment of indexes based on RF model.

Index Code	Index Name	Index Weight
I1	Precipitation during flood season (mm)	0.345
I2	Elevation (m)	0.054
I3	Urbanization rate (%)	0.039
I4	Population density (people/km^2)	0.025
I5	GDP per square kilometer of land (0.1 billion CNY/km^2)	0.049
I6	Per capita arable land area (10,000 people/km^2)	0.043
I7	Water area ratio (%)	0.039
I8	Vegetation coverage (%)	0.030
I9	Road network density in built-up areas (km/km^2)	0.027
I10	Direct economic losses from floods (10 million CNY)	0.298
I11	Municipal flood control investment per unit area (10,000 CNY)	0.051

3. Methodology

3.1. Research Framework

We developed a technical framework for analyzing the risk assessment and zoning of rain and flood hazards in Huangshan City (Figure 2).The corresponding framework consists of five modules: construction of evaluation indicators, determination of indicator weights, construction of the rainstorm and flood hazard risk assessment model, model validation, and policy decision-making. A DPSIR framework-based natural disaster risk indicator system is constructed in the first module. In the second module, complex nonlinear relationships among indicators are captured, and their comprehensive weights are calculated by the RF algorithm. In the third module, our research group sets up the flood hazard risk assessment model, involving hazard, vulnerability, exposure, and emergency response capacity. In this study, a flood hazard risk zoning map of Huangshan City is completed by combining the Soil Conservation Service (SCS) model with a Geographic Information System (GIS)-based spatial analysis. The accuracies of the flood risk assessment are validated in the fourth module by comparing the spatial distributions of flood hazard risk levels and the impacts by "7 July 2020". Lastly, policy recommendations developed from the assessment outcomes are formulated in the fifth module to support disaster prevention and mitigation efforts.

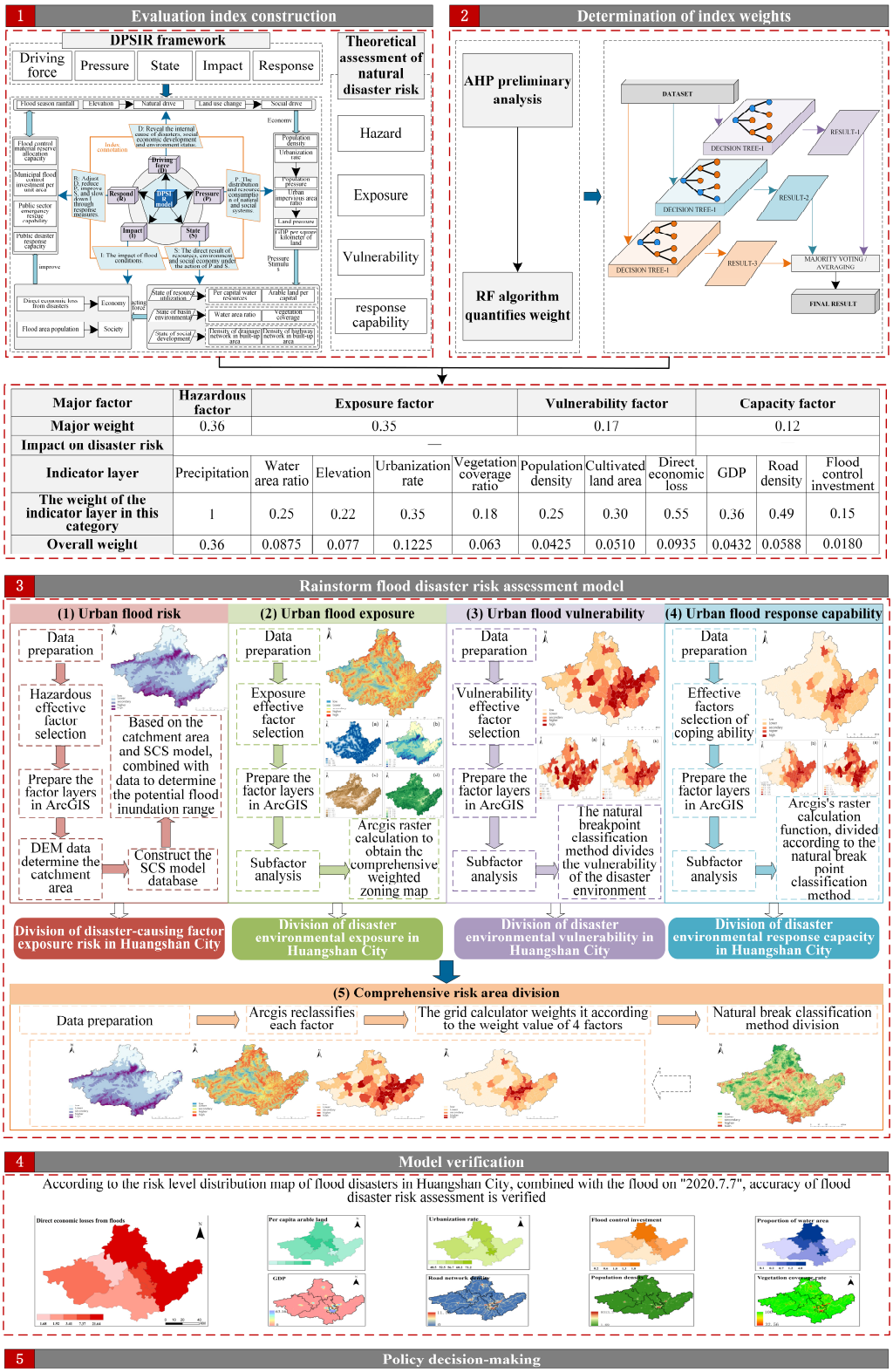

Major factor	Hazardous factor	Exposure factor				Vulnerability factor			Capacity factor		
Major weight	0.36	0.35				0.17			0.12		
Impact on disaster risk	—										
Indicator layer	Precipitation	Water area ratio	Elevation	Urbanization rate	Vegetation coverage ratio	Population density	Cultivated land area	Direct economic loss	GDP	Road density	Flood control investment
The weight of the indicator layer in this category	1	0.25	0.22	0.35	0.18	0.25	0.30	0.55	0.36	0.49	0.15
Overall weight	0.36	0.0875	0.077	0.1225	0.063	0.0425	0.0510	0.0935	0.0432	0.0588	0.0180

Figure 2. Research framework and technical ideas.

3.2. DPSIR Framework

Urban flood disasters are examples of socio-environmental problems, engaging socioeconomic conditions, environmental changes, land use planning, water environment management, and climate change. With the complex interactions among these factors, it is difficult to predict the probability and impacts of flood disasters, especially as climate change adds complexity to the system. Currently, flood risk assessment methodologies lack

standardized evaluation criteria, and there is no universally accepted framework for assessment indicators [37]. Given this issue, the Organization for Economic Co-operation and Development (OECD) introduced the Pressure-State-Response (PSR) framework [38], which describes the relationships between human activities, resource utilization, environmental changes, and management responses. Subsequently, the European Environment Agency (EEA) expanded this model into the DPSIR framework (Figure 3) [39,40], which emphasizes "Driving Forces" as direct influencing factors and distinguishes between "State" and "Impact" components. In this way, the analysis becomes more structured and systematic. DPSIR framework with the ability to analyze causal relations of multidimensional complex systems has been widely applied in environmental assessment (EE). Hence, the application of the DPSIR paradigm in the assessment of urban flood disasters effectively clarifies the interrelations of social, economic, ecological, and resource aspects. Such methodology lays an experimental foundation for the management of flooding risk, enables quantitative risk assessment, and assists in the formulation of prevention and mitigation strategies for disasters [41].

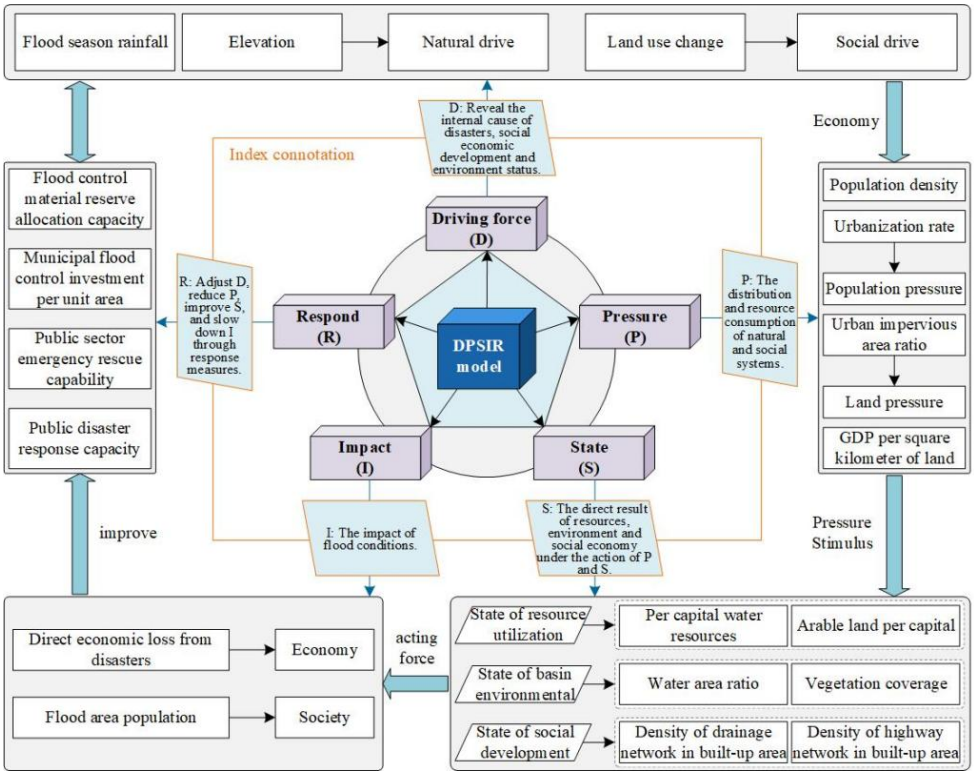

Figure 3. The conceptual framework of driving force, pressure, state, impact, and response (DPSIR).

3.3. Random Forest Algorithm

RF is a machine learning algorithm that performs classification or regression analysis by constructing multiple decision trees. It is one of the most accurate models for classification predictions, consisting of decision trees and the Bagging (Bootstrap Aggregating) algorithm [42]. Compared to other methods, RF has a lower generalization error and higher prediction accuracy, allowing it to be well suited for problems with no prior knowledge, nonlinear multivariable constraints, or incomplete datasets [43]. In this study, the RF algorithm adopts historical rainstorm and flood disaster data from Huangshan City while integrating multiple influencing factors for risk prediction. Each decision tree is trained on a different subset of the data, and the final prediction result is determined through a majority voting mechanism among all decision trees. The application of the RF algorithm enables

effective quantification and spatial evaluation of flood hazard risks so as to reinforce the accuracy and robustness of flood risk assessment [44].

During the data preparation stage, Bootstrap sampling is first conducted. This process involves randomly selecting multiple subsets from the original dataset with replacement and forming training sets. This procedure is repeated T times to generate T training subsets. In flood hazard prediction, information gain and the Gini index are commonly used as splitting criteria. Information gain measures the reduction in uncertainty (entropy) after a feature is split to identify the most critical factors contributing to flood occurrence [44]. The formula for information gain is expressed as the following:

$$\text{Information Gain(IG)} = \text{H(D)} - \sum_{\text{i=1}}^{\text{m}} \frac{\mid \text{D}_\text{i} \mid}{\mid \text{D} \mid} \text{H}(\text{D}_\text{i}) \tag{1}$$

where H(D) represents the uncertainty of dataset D; D_i denotes the subsets generated after splitting by a given feature; $\mid \text{D} \mid$ and $\mid \text{D}_\text{i} \mid$ embody the number of samples in the original dataset and the subset, respectively. The Gini index measures the impurity of a dataset, and its calculation formula is

$$Gini(D) = 1 - \sum_{i=1}^{k} p_i^2 \tag{2}$$

where p_i indicates the proportion of samples belonging to the ith class in the dataset, and k stands for the total number of classes. At each decision tree node, the feature that either minimizes the Gini index or maximizes information gain is selected in the Random Forest algorithm to perform data splitting.

Once the decision trees are trained, the model enters the ensemble learning stage. The Random Forest algorithm generates the final prediction by aggregating the results of multiple decision trees [45]. Suppose there are T decision trees, and each tree predicts the outcome $\hat{y}_t$ for a given sample x. Following a majority voting mechanism, the final prediction $\hat{y}$ is determined by selecting the class with the highest occurrence frequency, expressed as the following:

$$\hat{y} = majority\_vote\left(\hat{y}_1, \hat{y}_2, \ldots, \hat{y}_t\right) \tag{3}$$

For regression issues, the Random Forest algorithm determines the final prediction by computing the average of all decision trees' predictions, expressed as follows:

$$\hat{y} = \frac{1}{T} \sum_{t=1}^{T} \hat{y}t \tag{4}$$

The predictions of all decision trees are aggregated, and the final output is determined by voting (for classification) or averaging (for regression).

Regarding model evaluation, the Random Forest algorithm adopts out-of-bag (OOB) samples to assess performance. During training, some samples are not selected for a given decision tree and serve as OOB samples. These samples are employed for model validation, allowing for the computation of the OOB error. The formula for the OOB error rate is

$$OOB\ Error = \frac{1}{N_{OUT}} \sum_{i=1}^{N_{out}} II\left(\hat{y}_i^{out} \neq y_{out}\right) \tag{5}$$

where N_{out} represents the number of out-of-bag samples; $\hat{y}_i^{out}$ designates the predicted result for the i th out-of-bag sample; y_{out} describes the true label of that sample; II indicates

an indicator function that equals 1 if the predicted result differs from the true value and 0 otherwise.

Additionally, Random Forest can compute feature importance. The algorithm can assign an importance score to each feature by analyzing each feature's contribution to model performance during the tree-splitting process. Feature importance is generally calculated upon the decrease in the Gini index, expressed as the following:

$$Feature\ Importance_j = \sum_{t=1}^{T} \sum_{n \in t} \left(\frac{N_n}{N} \right) \Delta Gini_n \tag{6}$$

where N_n represents the number of samples in node n; $\Delta Gini_n$ denotes the decrease in the Gini index provoked by the splitting of feature j at node n; and N embodies the total number of samples. Through these calculations, Random Forest can identify the most influential features affecting flood hazard prediction results. This capability assists in effective feature selection and model optimization for flood risk assessment.

3.4. SCS-CN Model

The SCS-CN model (Soil Conservation Service Curve Number method) is a hydrological model utilized to estimate runoff volume based on factors such as rainfall, soil type, land use, and vegetation cover. In this study, the SCS-CN model is applied. Specifically, the Curve Number (CN) values to different regions of Huangshan City are assigned, and runoff volume is calculated based on rainfall data to assess flood risk. The fundamental equation is

$$Q = \frac{(P - I_a)^2}{P - I_a + S} \tag{7}$$

where Q represents the runoff volume (mm), which is the surface runoff generated by rainfall during a storm event; P denotes the precipitation (mm), indicating the total rainfall depth; and I_a embodies the initial abstraction, namely, the amount of rainfall intercepted, evaporated, or infiltrated by soil and vegetation before runoff occurs, typically assumed to be 20% of the potential maximum retention S, i.e., I_a = 0.2 S. Additionally, S stands for the potential maximum retention (mm), revealing the maximum amount of water that can be absorbed by soil and vegetation during a rainfall event. It is determined by the Curve Number (CN). The equation for S is

$$S = \frac{25,400}{CN} - 254 \tag{8}$$

where CN denotes the Curve Number, ranging from 0 to 100, indicating the combined effects of soil permeability, land use type, and vegetation cover within the watershed. A higher CN value suggests greater runoff generation and lower infiltration and retention capacity. Conversely, a lower CN value reflects that more rainfall is absorbed and intercepted by the soil, resulting in less runoff.

In this study, the SCS-CN model is applied to flood hazard risk assessment in Huangshan City. The model calculates runoff volumes for different areas by collecting regional precipitation data and integrating soil type, land use, and vegetation cover information. These calculations help identify flood-prone regions, providing a scientific basis for flood prevention and disaster response planning.

4. Results

4.1. Weighting of the Flood Hazard Evaluation Indicator System

As analyzed above, flood disasters stem from the interaction of multiple factors. In recent years, researchers have proposed various flood hazard evaluation indicator systems, typically incorporating factors such as precipitation intensity and frequency, meteorological conditions, hydrographic density, land use changes, population distribution, and infrastructure vulnerability. In this study, flood characteristics in Huangshan City, Anhui Province, are examined to analyze the influencing factors of flood subsystems from the perspectives of driving forces, pressures, states, impacts, and responses. Following this analysis, expert consultations are conducted, and then 11 indicators are selected for constructing the flood hazard evaluation system (Table 2). The selection of these indicators is based on the following considerations. First, Huangshan City experiences frequent and heavy rainfall, making precipitation intensity and annual rainfall crucial flood-inducing factors. Where there is a dense network of rivers and a large watershed coverage, the water basin covers a high area, and thus there are more users. It has high mountains and areas where water may accumulate, increasing the chances of flooding even more. Urbanization can change the capacity of water discharge, while flood control concrete (reservoir capacity, drainage) acts as a barrier to flooding. Furthermore, population density, vulnerability of infrastructure, and economic losses are included to evaluate the more general effects of floods concerning society and the economy. Through the combination of these factors, the multi-factor evaluation system provides a comprehensive assessment of flood hazard risk in Huangshan City.

In disaster risk assessment, the selection of evaluation indicators typically depends on four key assessment factors: hazard, exposure, vulnerability, and response capacity [46]. These factors reflect the probability of disaster occurrence, the affected population and assets, the extent of social and economic damage, and the ability of communities and governments to respond to disasters, respectively. With these four key factors, the 11 indicators selected by the DPSIR framework are categorized accordingly, and their weights are determined. In addition, indicators at the same level are compared in pairs to assign values upon their relative importance. The weight of each indicator is calculated through the Analytic Hierarchy Process (AHP) to ultimately derive the composite weights for different levels (Table 3) [36].

Table 3. Flood hazard risk assessment indicators and weights for Huangshan City.

Major Factor	Major Factor Weight	Impact on Flood Risk	Indicator Level	Indicator Weight Within Major Factor	Overall Weight
Hazard Factor	0.36	+	Precipitation	1	0.36
Exposure Factor	0.35	+	Water area ratio	0.25	0.0875
			Elevation	0.22	0.077
			Urbanization rate	0.35	0.1225
			Vegetation coverage	0.18	0.063
Vulnerability Factor	0.17	+	Population density	0.25	0.0425
			Arable land ratio	0.30	0.0510
			Direct economic losses	0.55	0.0935
Response Capacity Factor	0.12	−	GDP	0.36	0.0432
			Road network density	0.49	0.0588
			Municipal flood control investment per unit area	0.15	0.0180

Huangshan City's 2020 flood disaster data (training set) are analyzed by the Random Forest (RF) algorithm to effectively measure the significance of each indicator in flood hazard assessment and to construct a more scientific urban flood risk evaluation system. The RF model training parameters include the number of classification trees and node branches. As the number of trees increases, the model becomes more stable. As suggested through multiple rounds of testing, the model achieves optimal performance when the number of classification trees is set to 300 and the number of node branches is set to three.

As revealed by analyzing the contribution of each factor to flood hazard risk, precipitation during the flood season and direct economic losses from disasters exhibited the strongest significance and had the greatest impact. In contrast, elevation, urbanization rate, GDP, per capita arable land area, water area ratio, vegetation coverage, and municipal flood control investment per unit area were of relatively lower importance (Figure 4). Moreover, urban flood disasters were less influenced by population density and road network density in built-up areas, with their combined impact on actual flood risk accounting for less than 10%.

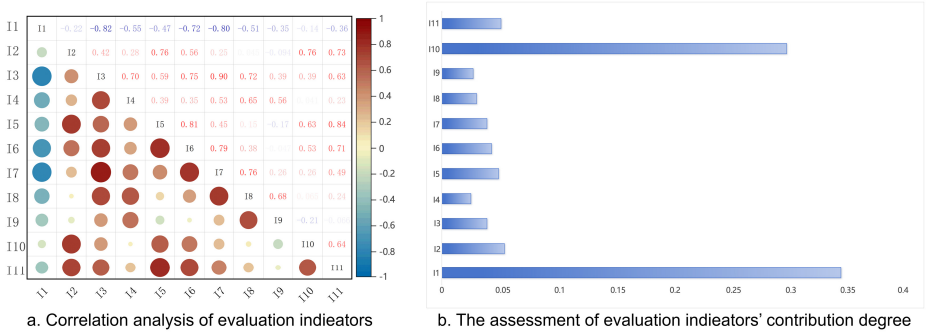

a. Correlation analysis of evaluation indieators b. The assessment of evaluation indieators' contribution degree

Figure 4. The importance of rainfall disaster index in Mount Huangshan City based on the Stochastic Forest Model.

4.2. Hazard Analysis Results

Watershed delineation and SCS model results, as well as historical rainfall data, river network information, and hydrological records, demonstrate that the potential flood inundation areas were identified, and risk levels were classified (Figure 5). The flood inundation risk was categorized into five levels: high risk, moderately high risk, moderate risk, moderately low risk, and low risk.

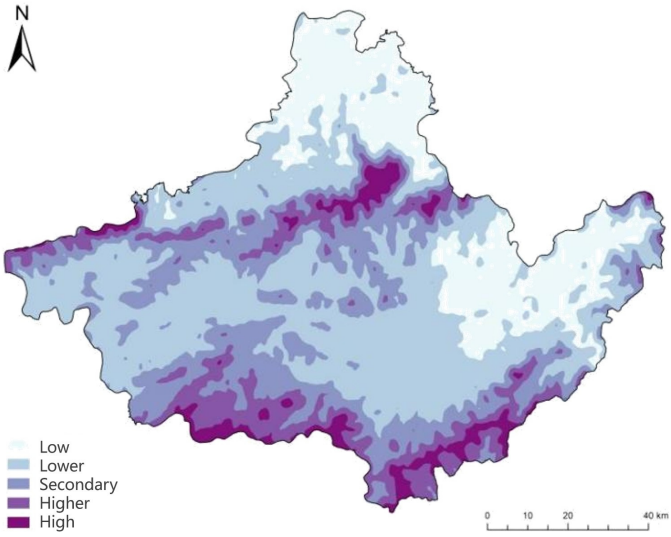

Figure 5. Risk division of disaster-causing factors in Huangshan City.

4.3. Exposure Analysis Results

With precipitation, water body proximity, slope, and vegetation coverage as weighted indicators, the raster calculation function in ArcGIS (10.8) was applied to generate a comprehensive weighted zoning map. Afterward, the Natural Breaks (Jenks) classification method was employed to categorize Huangshan City's environmental exposure to flood hazards into five levels: low exposure, moderately low exposure, moderate exposure, moderately high exposure, and high exposure (Figure 6).

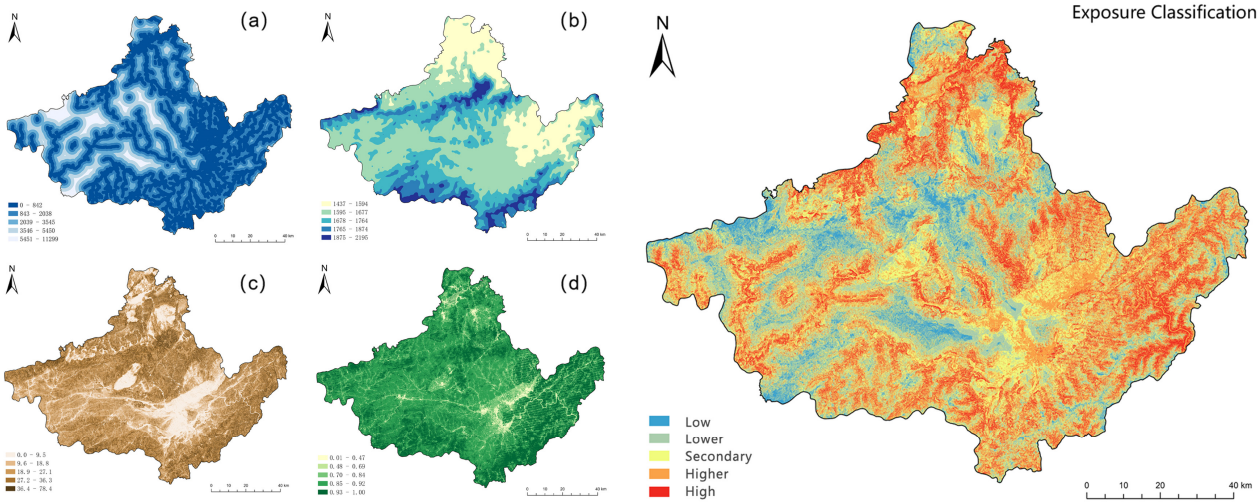

Figure 6. Division of disaster environmental exposure in Huangshan City. ((**a**). water body proximity, (**b**). precipitation, (**c**). elevation, (**d**). vegetation coverage).

4.4. Vulnerability Analysis Results

With population density and arable land ratio as the primary indicators, the raster calculation function in ArcGIS 10.8 was applied for weighted overlay analysis. By the Natural Breaks (Jenks) classification method, the vulnerability of the disaster environment was categorized into five levels: low vulnerability, moderately low vulnerability, moderate vulnerability, moderately high vulnerability, and high vulnerability (Figure 7).

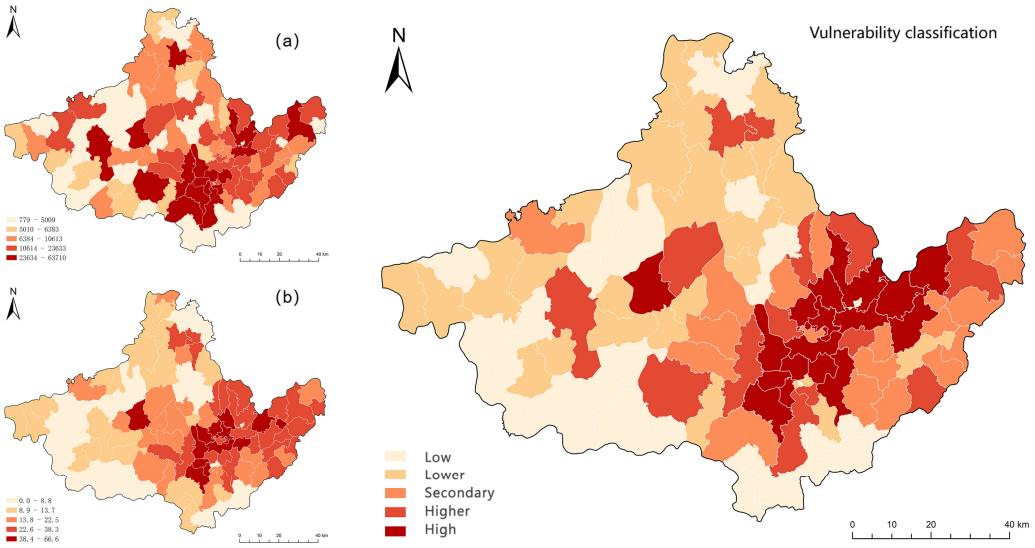

Figure 7. Division of disaster environmental vulnerability in Huangshan City. ((**a**). Population density, (**b**). arable land ratio).

4.5. Response Capacity Analysis Results

With per capita GDP and road network density distribution data for Huangshan City, the raster calculation function in ArcGIS 10.8 was applied to perform weighted overlay analysis. By the Natural Breaks (Jenks) classification method, the disaster prevention and mitigation capacity were categorized into five levels (Figure 8).

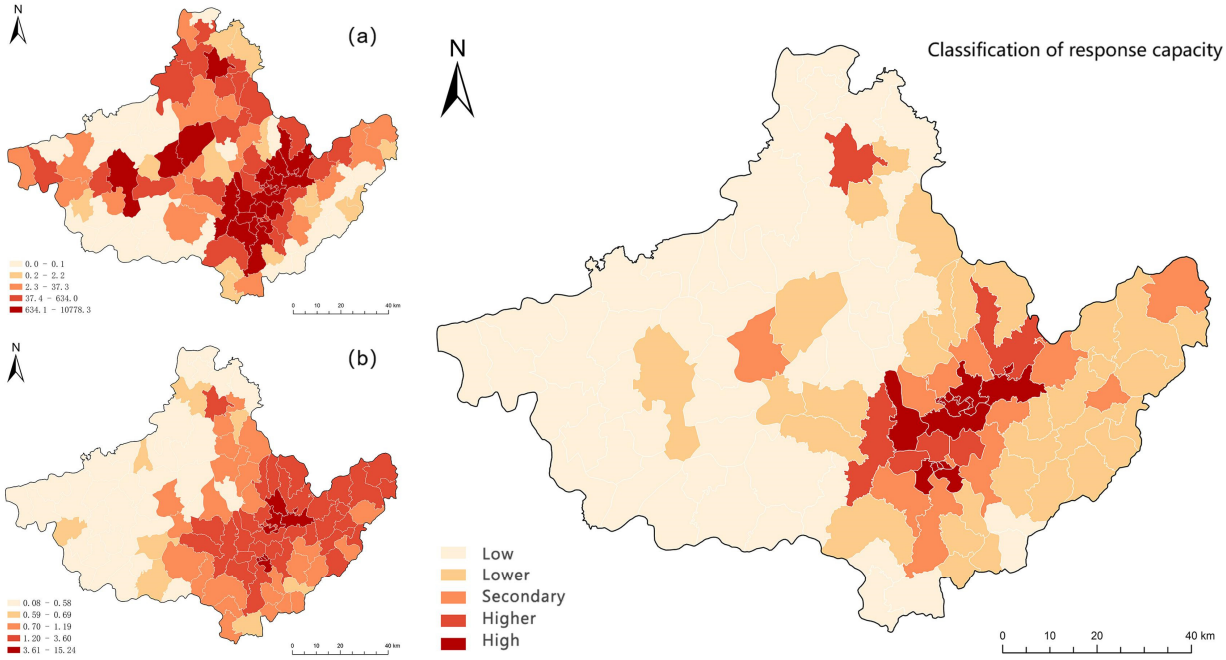

Figure 8. Division of disaster environmental response capacity in Huangshan City. ((**a**). per capita GDP, (**b**). road network density distribution).

4.6. Comprehensive Rainstorm and Flood Hazard Analysis Results

With the flood hazard risk assessment model and the weighted comprehensive evaluation method, the four assessment factors were assigned weights and combined through weighted calculation. Finally, the rainstorm and flood hazard risk levels in Huangshan City were classified into five levels (Figure 9) [47].

4.7. Validation of the Flood Risk Assessment Model Accuracy

The accuracy of the flood hazard risk assessment was verified by comparing the spatial distribution of flood risk levels in Huangshan City (Figures 5–9) with the impact of the "7 July 2020" flood event (Figure 10) [48]. Significant variations in flood risk levels across different regions of Huangshan City can be observed from the "Direct Economic Loss Distribution Map" (top-left corner of Figure 10). Among them, the northern areas of Huangshan District, Huizhou District, and Shexian County (deep red areas) suffered the most severe economic losses, reaching a value of 21.64, which was markedly higher than that in other regions. This distribution closely aligns with the spatial patterns of other influencing factors, further validating the reliability of the flood risk assessment model.

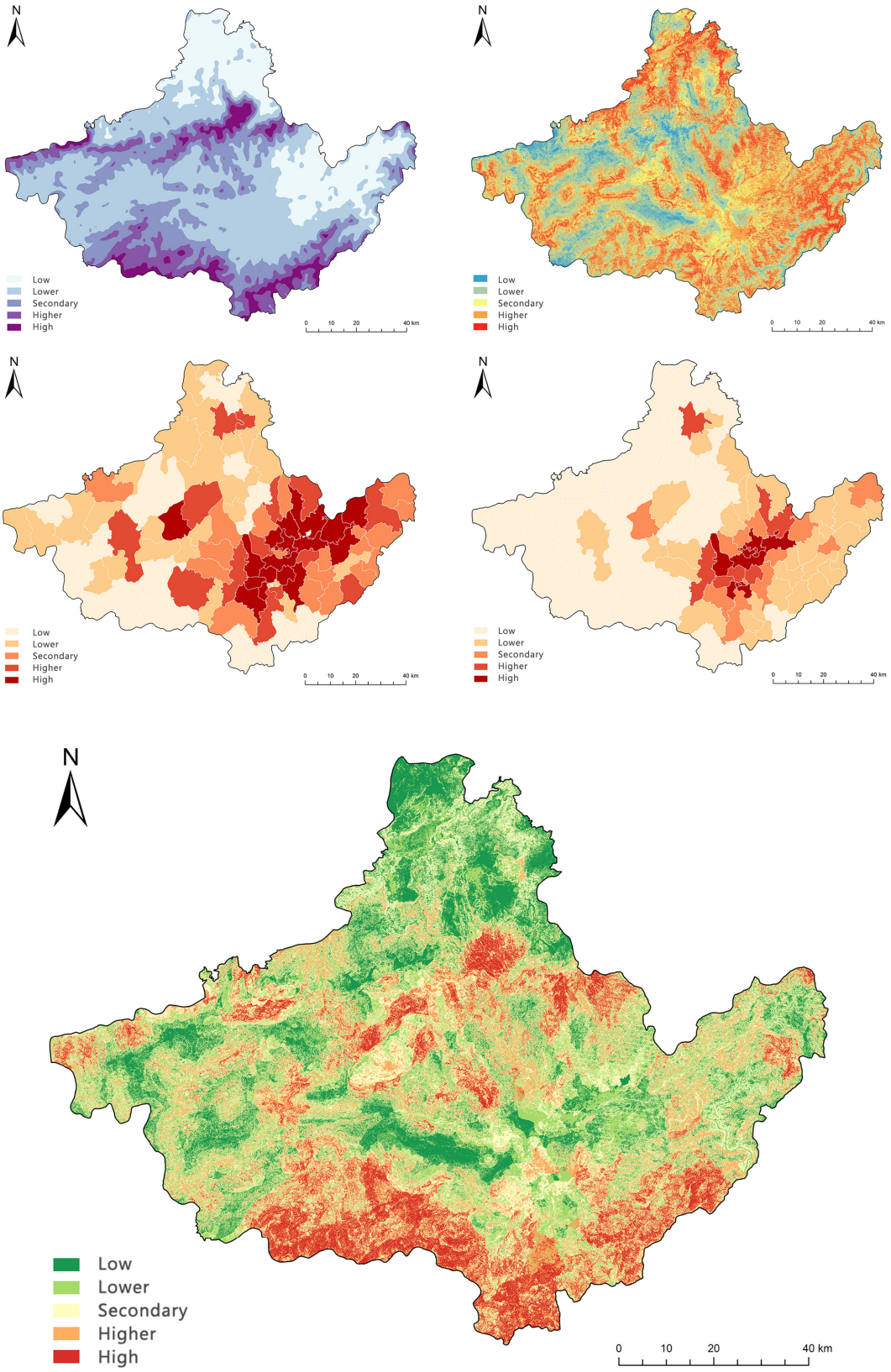

Figure 9. Comprehensive division of rain and flood disasters in Huangshan City.

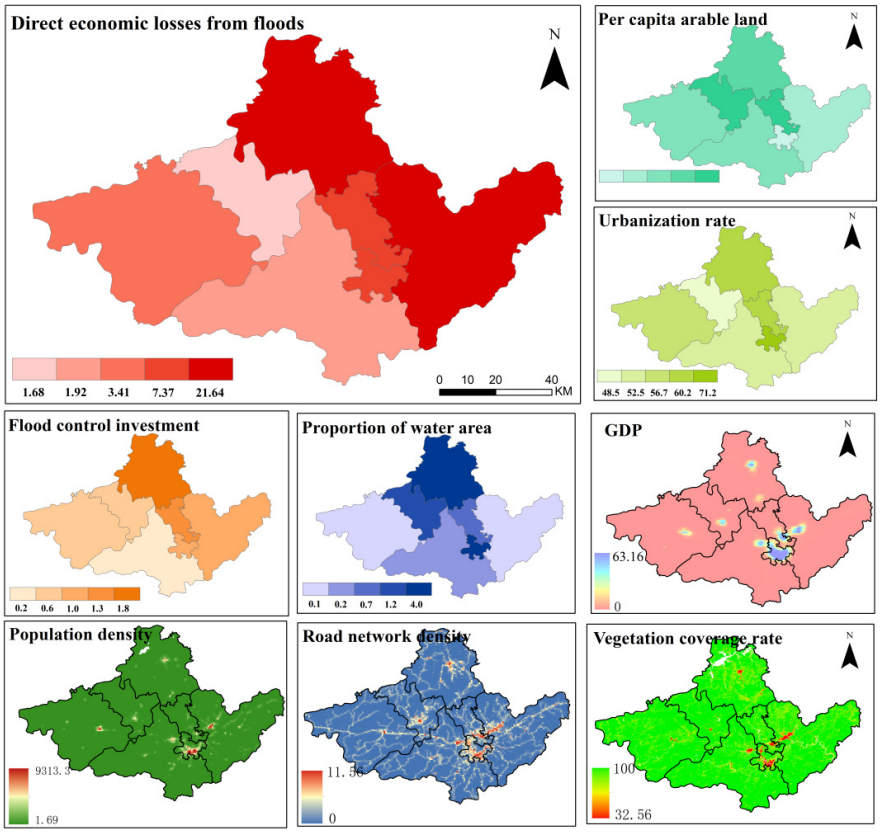

Figure 10. Spatial distribution of flood disaster factors in Huangshan City in 2020.

5. Discussion

5.1. Results of Random Forest Algorithm and SCS-Based Rain and Flood Hazard Risk Assessment and Zoning

Hazard analysis is a core step in flood risk assessment and zoning using GIS and the SCS model. First, a Digital Elevation Model (DEM) was used to delineate watersheds within the study area. Watershed analysis was conducted through the hydrological analysis module in GIS, and Huangshan City was divided into six watersheds [36].

Next, an SCS model database was established. The CN values corresponding to different areas in Huangshan City were determined following the Curve Number (CN) lookup table from the SCS model (Table 4). Additionally, the 5-year, 10-year, 20-year, 50-year, and 100-year return period rainfall amounts were calculated as 80.2 mm, 98.6 mm, 118.5 mm, 144.7 mm, and 165.8 mm, respectively, based on the Pearson Type III distribution curve [36]. The area-weighted average CN value for each watershed was calculated with the rainfall data for different return periods and the six delineated watersheds in Huangshan City. Finally, with the runoff calculation formula from the SCS model, the rainwater runoff volume, and total water volume for each watershed were determined by the corresponding CN values and rainfall data for different return periods.

Table 4. SCS model parameters.

Soil Type	Farmland	Grassland	Forest	Urban Built-Up Area
Type A Soil	65	39	30	77
Type B Soil	75	61	55	85
Type C Soil	83	74	70	90
Type D Soil	87	80	77	95

The hazard classification was obtained from the watershed delineation and SCS model results. The analysis suggests that moderate-risk areas account for 26.64%, while moderately high-risk areas occupy 14.23%. High-risk areas have the smallest proportion of 4.86% and are mainly distributed in southern Xiuning County and Shexian County, as well as northern Qimen County and central Yixian County. Low-risk areas account for 23.83%. Flood inundation zones are concentrated along the Xin'an River Basin, primarily affecting Tunxi District, Shexian County, Qimen County, Xiuning County, and Yixian County.

Additionally, exposure analysis was conducted. Proximity to water bodies is a key indicator for evaluating flood exposure because areas near rivers and water bodies are more vulnerable to flooding, especially during heavy rainfall or rising river levels. With ArcGIS 10.8, buffer zones for major rivers and lakes in Huangshan City were generated to create a water body proximity distribution map (Figure 6a). The results imply that Xiuning County and Yixian County are primarily located near rivers and water bodies, allowing them to be more susceptible to flood impacts during heavy rainfall events. Furthermore, precipitation levels were analyzed as another critical factor. Figure 8b demonstrates that the southern and central parts of Huangshan City are subject to significant precipitation, leading to their increased flood risk potential.

Slope directly influences rainfall runoff velocity and accumulation processes. A slope distribution map was generated by slope analysis (Figure 6c). The results unveil that central Huangshan City, as well as parts of the southeastern and northern regions, have relatively low slopes and are close to rivers. These areas are vulnerable to increased river levels and subsequent flooding during long periods of rainfall. In contrast, southern parts, especially Shexian County and Qimen County, have more pedestrians and greater susceptibility to flash floods and debris flow owing to steep slopes.

Lastly, the distribution of vegetation coverage is also crucial in the retention of soil water and the formation of floods. Areas with good vegetation are adopted to reduce surface runoff, assisting in mitigating the risk of flooding. Meanwhile, areas with little vegetation are more susceptible to flooding. An NDVI distribution map was generated by calculating the Normalized Difference Vegetation Index (NDVI) from remote sensing imagery (Figure 6d). Huangshan City maintains a relatively high vegetation coverage rate and good vegetation, which can protect the soil, maintain water and soil, and regulate the hydrological process. Nevertheless, complex terrain, soil saturation, and other conditions play a counterproductive role in the regional cover vegetation, so as to exacerbate flood disaster risk.

As exhibited in the exposure classification map (Figure 6), moderate-high-risk and high-risk areas are mainly concentrated in the southeastern, northern, and part of the central region of Huangshan City, which is included in Qimen County, Shexian County, and Huangshan District. With a dense river network and relatively low slopes, these areas are very sensitive to prompt flood disasters.

Furthermore, the vulnerability analysis was conducted. The vulnerability of the affected areas is directly proportional to population density and the proportion of cultivated land [36]. Figure 7a,b illustrate the distribution of population density and cultivated land ratio in Huangshan City. As observed from the vulnerability classification map (Figure 7), areas with high and relatively high vulnerability are primarily concentrated in the southeastern part of Huangshan City, including Tunxi District, Shexian County, and Huizhou District. These areas have high population density and a larger proportion of cultivated land. From another perspective, regions with low and relatively low vulnerability are located in the northern and southwestern parts of the city, where population density is low and cultivated land proportion is smaller, such as Qimen County, Yi County, and Huangshan District.

Finally, the response capacity was analyzed with per capita GDP and road density as quantitative variables that can indicate the capacity of the university region to respond to disasters in relevant forms such as infrastructure and economic circumstances. The stronger the ability to provide economic support for disaster response, the higher the per capita GDP, and the denser the road network, contributing to improving disaster prevention and mitigation capacity. In Huangshan City, per capita GDP and road density distributions are plotted in Figure 8a,b. The response capacity classification map (Figure 8) demonstrates that regions such as Tunxi District, Huizhou District, and parts of Qimen County and Yi County have higher per capita GDP and denser road networks, indicating a strong disaster response capacity. In contrast, the southeastern part of Shexian County and most of the western areas of Huangshan City are economically underdeveloped, with relatively weaker infrastructure and poor disaster response capacity.

After the quantitative analysis of the four evaluation factors, each factor was reclassified by ArcGIS 10.8. With the disaster risk evaluation model and the weighted comprehensive evaluation method, the raster calculator was employed to perform weighted calculations according to the weights of the four factors. By the Natural Breaks classification method, the rainstorm flood disaster risk in Huangshan City is classified into five levels: low risk, low-medium risk, medium risk, high-medium risk, and high risk (Figure 11).

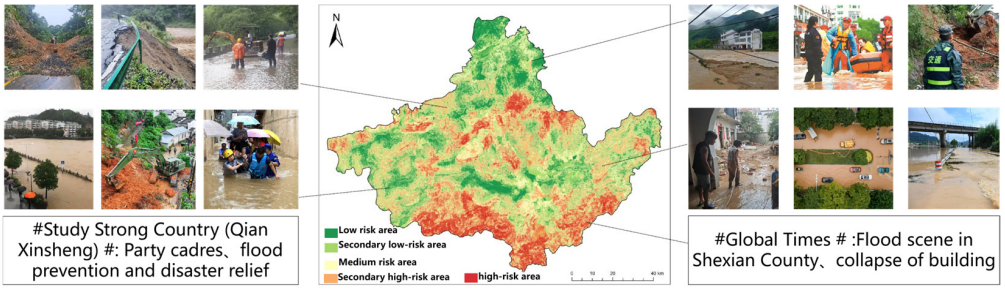

Figure 11. Disaster topic in each county.

5.2. Regulation Countermeasures

The severity of urban flood disasters is closely related to factors such as rainfall, topography, economic level, land use, flood control investment, and emergency capabilities. A single flood control strategy is insufficient to address complex environmental challenges. Modern flood management emphasizes basin water resource planning and multi-level policy coordination [49]. Countries such as the Netherlands and Mexico are exploring new models of integrated flood management [19,50] while advocating for flood control measures that align with the principle of multi-dimensional, multi-factor coordinated development across social, economic, and ecological domains. Through the flood disaster risk assessment results for Huangshan City, this study effectively reduces flood risks in Huangshan City by improving urban infrastructure, promoting regional ecological and economic development, and strengthening disaster prevention and emergency rescue capabilities [51].

Firstly, infrastructure improvements in Huangshan City suggest that factors such as municipal flood control investment and vegetation coverage significantly impact urban waterlogging. Drainage facilities should be built to form a rainwater drainage system in Huangshan City with converging pipelines, pumping stations, and other facilities to pump out excess water. In addition, a drainage well with city storm drainage should be repaired to ensure that drainage is unobstructed. Impervious surface coverage should be limited. Permeable pavements and building materials as well as reductions in hardened areas should be encouraged. Moreover, it is also a response to sponge city, which advocates for the development of green infrastructure featuring permeable surfaces, greenways, watercourses,

and wetlands to improve flood control and drainage. Furthermore, it is a cross-disciplinary work that should cooperate with various sectors to safeguard the ecosystem.

Per capita GDP, population density, urbanization rate, land use, and other indicators are important for the coordination of the economy and ecology regarding the sustainable development of the economy and ecology in regions. As a resources-based city, Huangshan is more confronted with the contradiction of eco-protection and econo-development, which requires green development and ecological civilization. The government must promote unique industries including eco-tourism, agriculture, and green industries. They will also facilitate regional economic connections by enhancing transport links to surrounding cities and strengthening transportation in mountain and remote areas. Flooding will become more severe because of urban sprawl with increasing land development pressure. Thus, reasonable land use planning should be implemented, and large-scale development of flood-prone areas should be avoided. Urban waterlogging can potentially be avoided through adequate land-use planning and better drainage systems [52].

Concerning ecological protection, the mountainous areas are ecologically fragile, with severe soil erosion and overdevelopment in some regions. The government should intensify ecological restoration efforts by converting farmland to forests, planning ecological land use carefully, combating soil erosion, and focusing on green development. Optimizing infrastructure and industrial layout will contribute to sustainable development and effective flood disaster prevention. Factors such as rainfall during the flood season, low-lying topography, and emergency response capabilities are critical in disaster prevention and response. At present, non-structural flood control measures in Huangshan are underdeveloped, particularly in addressing sudden urban waterlogging events. It is necessary to strengthen waterlogging monitoring and early warning systems, develop real-time monitoring platforms, and improve public awareness and self-rescue capabilities. The government should also enhance the emergency management system, promote inter-departmental collaboration, and invest in infrastructure development in flood-prone areas to better manage extreme weather events. Huangshan City can effectively reduce flood risks and safeguard the lives and property of its citizens by improving emergency management, disaster monitoring, and public disaster preparedness.

6. Conclusions

In 2021, the People's Government of Anhui Province approved the Huangshan City Land Spatial Master Plan (2021–2035), marking a new phase in the accelerated urban integration of Huangshan. However, the city is encountering increasing pressure in flood disaster management with global climate change and rapid urbanization. In this study, a flood disaster risk management system was constructed based on the DPSIR framework, and Random Forest analysis was performed to identify 11 key indicators for assessing flood risk in Huangshan. GIS and the SCS model were applied for zoning and verification, and the "7 July 2020" flood event served as a case study to validate the accuracy of the model's results. The assessment results are presented by ArcGIS. The main research conclusions are summarized as follows.

The findings suggest that seasonal rainfall and topographical diversity are the primary driving factors for flood disasters in Huangshan, particularly in low-lying areas where heavy rainfall generally induces severe waterlogging. The conflict between population growth and land resource scarcity has intensified with the acceleration of urbanization. Flood risks are aggravated by the slow construction of flood control infrastructure and low drainage capacity. Additionally, there are still weak flood control capabilities in small and medium-sized rivers in the Huangshan watershed, and the slow construction of flood detention areas has not effectively mitigated flood disasters.

Three main methods were proposed to prevent and reduce the risk of flood disasters: (1) optimizing urban infrastructure, reflecting that drainage systems should be improved and maintained to strengthen the flood control capacity of the city; (2) promoting regional ecological economic development, indicating that peasants should be supported for their investments in ecological agriculture and that local eco-tourism should be promoted to increase green areas and help optimize the urban ecological environment; (3) strengthening disaster prevention and emergency response mechanisms, implying that emergency response plans should be revised to improve response capabilities and optimize resource allocation.

In the future, with the advancement of data technology and climate models, research can further expand evaluation indicators by incorporating factors such as land use changes, soil types, and long-term climate trends, while exploring advanced methods like deep learning to improve the accuracy of risk prediction and the interpretability of mechanisms. Urban planners can utilize the research findings to optimize the design of drainage systems and flood control infrastructure. Environmental scientists can build on the assessment methods to study the impacts of climate change. Emergency management personnel can refine contingency plans and response mechanisms, while policymakers can formulate scientifically informed flood control policies based on the conclusions.

However, this study has certain limitations. First, the selection of evaluation indicators remains somewhat constrained. Additional factors, such as land use changes, soil types, and long-term climate change trends, should be considered in future research to enhance the comprehensiveness and accuracy of the assessment. Second, the Random Forest and SCS-CN models, though they performed well in risk evaluations, have limitations in revealing the underlying mechanisms of flood occurrence. Thus, more advanced machine learning techniques, such as deep learning, could be explored in future studies to improve the accuracy of risk predictions and the explanatory power of flood mechanisms. With the continuous advancement of data technology and climate models, these limitations should be overcome to more precisely support flood disaster risk management in Huangshan.

Author Contributions: Conceptualization, Z.X. and B.S.; methodology, Z.X.; software, Z.X.; validation, Z.X. and B.S.; formal analysis, Z.X.; investigation, Z.X.; resources, B.S.; data curation, Z.X.; writing—original draft preparation, Z.X.; writing—review and editing, Z.X.; visualization, Z.X.; supervision, B.S.; project administration, Z.X.; funding acquisition, B.S. All authors have read and agreed to the published version of the manuscript.

Funding: Sichuan Provincial Science and Technology Department Key Project: Research and Demonstration on Suitability Planning of Green and Livable Village and Town Settlement in South Sichuan Region Based on Disaster Avoidance Perspective (2020YFS0309).

Data Availability Statement: https://www.webmap.cn/main.do?method=index (accessed on 11 September 2024); https://data.cma.cn/ (accessed on 11 September 2024); https://www.fao.org/soils-portal/en/ (accessed on 11 September 2024); https://sthjj.huangshan.gov.cn/ (accessed on 11 September 2024); https://tjj.huangshan.gov.cn/ (accessed on 15 September 2024); http://www.moa.gov.cn/ (accessed on 15 September 2024); https://slj.huangshan.gov.cn/ (accessed on 15 September 2024).

Conflicts of Interest: The authors declared that they have no conflicts of interest.

Appendix A

Table A1. Historical Flood Disaster Statistics in Huangshan City.

Event	Time	Impact Description
1954 Flood	May–July	Rainfall reached 1620 mm, accounting for 67% of the annual total. Affected 256 townships in Huizhou Prefecture, with a disaster area of 147,000 mu. Destroyed 3068 hydraulic engineering structures and 710 houses, washing away 52,000 cubic meters of timber. The peak flood response involved 61,000 people.
"5 July 1969" Flood	July	The most severe flood disaster in Huizhou Prefecture since the founding of the People's Republic of China. The flood affected 252,000 mu of land, with peak flood response mobilization reaching 183,100 people. Shexian County suffered the most severe losses, including damage to ancient bridges and the destruction of several hydraulic projects, such as the Lianchuan Reservoir.
July 1991 Flood	July	Concentrated around the Huangshan area, where the scenic region experienced an exceptionally rare torrential downpour, with cumulative rainfall exceeding 700 mm in seven days. Yixian County recorded the second-highest rainfall, ranging from 500 to 700 mm.
July 1996 Flood	June–July	The entire city experienced extreme rainfall, with precipitation exceeding 450 mm in all areas. The highest recorded rainfall was 663 mm in Sanyang, Shexian County, followed by 602 mm in Jilian, Yixian County, 568 mm in Qimen County, and 583 mm in Huangshan District. Extensive flooding along both banks of the Xin'an River.
May 2006 Flood	May–May	A once-in-50-year torrential rain event affected 670,000 people and caused direct economic losses of 366 million yuan.
June 2011 Flood	June–June	Four consecutive heavy rainfall events led to an average citywide precipitation of 661.1 mm. The heaviest rainfall occurred in southern Xiuning County (Wangcun, Banqiao, Chenxia, Tunxi, and Wangcun in Shexian County). The highest recorded station, Banqiao Town in Xiuning, reached 959.7 mm, with eight other stations exceeding 800 mm.
"30 June 2013" Flood	June	The flood center was located upstream of Fengle Reservoir in Huizhou District. Affected 133,000 people citywide. Torrential rains caused 10 reservoirs, including Fengle Reservoir, to exceed flood control limits, with six reservoirs overflowing. Mountain floods and landslides occurred in Huizhou District, leading to severe damage.
"7 July 2020" Flood	June–July	The city endured five consecutive heavy rain and flood events, with precipitation reaching 2.2 times the historical average for the same period. The 484-year-old Zhenhai Bridge (Old Bridge) in Tunxi was severely damaged by floodwaters. Shexian County experienced a once-in-50-year flood event, trapping over 1000 students in various parts of the county, leading to the postponement of the Chinese and Mathematics Gaokao exams originally scheduled for July 7.
"20 June 2024" Flood	June–June	Huangshan City upgraded its flood emergency response to Level II. Over 206,000 people were affected, with 164,000 mu of farmland suffering flood damage.

References

1. Guo, Q.; Jiao, S.; Yang, Y.; Yu, Y.; Pan, Y. Assessment of urban flood disaster responses and causal analysis at different temporal scales based on social media data and machine learning algorithms. *Int. J. Disaster Risk Reduct.* **2025**, *117*, 105170. [CrossRef]
2. Wang, D.; Chen, B.K. The historical origin of social participation in public infrastructure: Evidence from rural water conservancy construction. *World Econ.* **2024**, *47*, 151–183. [CrossRef]
3. Wan, Z.W.; Tang, C.C.; Xu, H. Research review and outlook on achieving the "dual carbon" goals for tourism destinations. *Tour. Trib.* **2025**, 1–22. [CrossRef]
4. Delleur, J.W.; Dendrou, S.A.; McPherson, M.B. Modeling the runoff process in urban areas. *Crit. Rev. Environ. Sci. Technol.* **1980**, *10*, 1–64. [CrossRef]
5. Liu, Y.Q.; You, M.; Zhu, J.L.; Wang, F.; Ran, R.P. Integrated risk assessment for agricultural drought and flood disasters based on entropy information diffusion theory in the middle and lower reaches of the Yangtze River, China. *Int. J. Disaster Risk* **2019**, *38*, 101194. [CrossRef]
6. Tian, Y.; Ma, J.; Yue, Q.R.; Xu, Z.; Lu, X.Z.; Zhang, M.L.; Gu, D.L.; Lu, M.T. Analysis of the 2024 Noto Peninsula earthquake based on the urban safety "risk source-disaster body-reduction capacity" theory. *Eng. Mech.* **2022**. [CrossRef]
7. Zhou, Y.L.; Bai, Y. Exploration and enlightenment of community disaster emergency services in American public libraries. *Libr. Constr.* **2021**, *8*, 151–161. [CrossRef]
8. Jia, Y.H.; Bai, Y.; Zhai, L.X. Rainstorm and flood disaster risk assessment in Guangxi based on AHP-entropy method. *Surv. Spat. Geogr. Inf.* **2023**, *10*, 13–17.
9. Tang, L.Y.; Zhao, Y.H.; Zhang, H. Agricultural flood disaster risk assessment model based on GIS in the Sanjiang Plain. *Heilongjiang Agric. Sci.* **2023**, *9*, 98–104.
10. Kabenge, M.; Elaru, J.; Wang, H.; Li, F.T. Characterizing flood hazard risk in data-scarce areas, using a remote sensing and GIS-based flood hazard index. *Nat. Hazards* **2017**, *89*, 1369–1387. [CrossRef]
11. Islam, M.M.; Sado, K. Flood hazard assessment in Bangladesh using NOAA AVHRR data with geographical information system. *Hydrol. Process.* **2015**, *14*, 605–620. [CrossRef]
12. Burton, I.; Cates, R.W.; White, G.F. The Environment as Hazard. *Geogr. J.* **1979**, *145*, 126–129.
13. Sun, N.; Li, C.; Guo, B.Y.; Sun, X.K.; Yao, Y.K.; Wang, Y. Urban flooding risk assessment based on FAHP–EWM combination weighting: A case study of Beijing. *Geomat. Nat. Hazards Risk* **2023**, *14*, 2240943. [CrossRef]
14. Wang, G.; Liu, Y.; Hu, Z.; Lyu, Y.; Zhang, G.; Liu, J.; Liu, Y.; Gu, Y.; Huang, X.; Zheng, H.; et al. Flood Risk Assessment Based on Fuzzy Synthetic Evaluation Method in the Beijing-Tianjin-Hebei Metropolitan Area, China. *Sustainability* **2020**, *12*, 1451. [CrossRef]
15. He, X.Y.; Tian, W.C.; Zhang, Z.Y.; Liao, Z.L. Research progress on data-driven flood risk assessment methods. *People's Pearl River* **2022**, *43*, 60–67.
16. Zhang, Q.Y.; Xu, Y.P.; Lei, C.G.; Wang, Y.F.; Han, L.F. Flood risk assessment of downstream areas of reservoirs in the southeastern coastal region based on dynamic simulation. *Lake Sci.* **2016**, *28*, 868–874.
17. Nie, C.J.; Ye, H.C.; Zhang, S.W.; Guo, J.W.; Cui, B.; Huang, W.J. Agricultural typhoon disaster risk assessment and sustainable development strategies for Hainan Island. *Trans. Chin. Soc. Agric. Eng.* **2022**, *38*, 237–246.
18. Su, J.S.; Zhang, B.F.; Xu, X. Advances in machine learning based text categorization. *Ruan Jian Xue Bao (J. Softw.)* **2006**, *17*, 1848–1859. [CrossRef]
19. Chen, J.F.; Li, Q.; Wang, H.M.; Deng, M.H. A machine learning ensemble approach based on random forest and radial basis function neural network for risk evaluation of regional flood disaster: A case study of the Yangtze River Delta, China. *Int. J. Environ. Res. Public Health* **2019**, *17*, 49. [CrossRef]
20. Anderson, D.L.; Ruggiero, P.; Mendez, F.J.; Barnard, P.L.; Erikson, L.H.; O'Neill, A.C.; Merrifield, M.; Rueda, A.; Cagigal, L.; Marra, J. Projecting Climate Dependent Coastal Flood Risk with a Hybrid Statistical Dynamical Model. *Earth's Future* **2021**, *9*, e2021EF002285. [CrossRef]
21. Wang, Z.L.; Lai, C.G.; Chen, X.H.; Yang, B.; Zhao, S.W.; Bai, X.Y. Flood Hazard Risk Assessment Model Based on Random Forest. *J. Hydrol.* **2015**, *527*, 1130–1141. [CrossRef]
22. Hao, M.M.; Jiang, D.; Ding, F.Y.; Hu, J.Y.; Chen, S. Simulating Spatio-Temporal Patterns of Terrorism Incidents on the Indochina Peninsula with GIS and the Random Forest Method. *ISPRS Int. J. Geo-Inf.* **2019**, *8*, 133. [CrossRef]
23. Amatya, D.M.; Walega, A.; Callahan, T.J.; Morrison, A.; Vulava, V.; Hitchcock, D.R.; Williams, T.M.; Epps, T. Storm Event Analysis of Four Forested Catchments on the Atlantic Coastal Plain Using a Modified SCS-CN Rainfall-Runoff Model. *J. Hydrol.* **2022**, *608*, 127772. [CrossRef]
24. Esfandiari, M.; Abdi, G.; Jabari, S.; McGrath, H. Flood Hazard Risk Mapping Using a Pseudo Supervised Random Forest. *Remote Sens.* **2020**, *12*, 3206. [CrossRef]

25. Chen, W.; Li, Y.; Xue, W.; Shahabi, H.; Li, S.J.; Hong, H.Y.; Wang, X.J.; Bian, H.Y.; Zhang, S.; Pradhan, B.; et al. Modeling Flood Susceptibility Using Data-Driven Approaches of Naïve Bayes Tree, Alternating Decision Tree, and Random Forest Methods. *Sci. Total Environ.* **2020**, *701*, 134979. [CrossRef] [PubMed]
26. Xu, Z.X.; Chu, Q.; Wang, H.; Ye, C.L. Research Progress on Urban Rainwater and Flood Simulation Technology Based on Land-Atmosphere Coupling. *J. Beijing Normal Univ. Nat. Sci.* **2022**, *58*, 434–446.
27. Jia, M.Y.; He, D.; Huo, X.W.; Zhang, H.R.; Jia, S.H.; Zhang, J. Exploring the Impact of Climate Change on Flood Risk at Cultural Heritage Sites Using a GIS-Based SCS-CN Method: A Case Study of Shanxi Province, China. *Int. J. Disaster Risk Reduct.* **2023**, *96*, 103968. [CrossRef]
28. Fang, Z.H.; Song, S.X.; He, C.Y.; Liu, Z.F.; Qi, T. Evaluating the Impacts of Future Urban Expansion on Surface Runoff in an Alpine Basin by Coupling the LUSD-Urban and SCS-CN Models. *Water* **2020**, *12*, 3405. [CrossRef]
29. El-Bagoury, H.; Gad, A. Integrated Hydrological Modeling for Watershed Analysis, Flood Prediction, and Mitigation Using Meteorological and Morphometric Data, SCS-CN, HEC-HMS/RAS, and QGIS. *Water* **2024**, *16*, 356. [CrossRef]
30. Al-Ghobari, H.; Dewidar, A.; Alataway, A. Estimation of Surface Water Runoff for a Semi-Arid Area Using RS and GIS-Based SCS-CN Method. *Water* **2020**, *12*, 1924. [CrossRef]
31. Zhao, X.; Zhang, L.; Zhu, X. Runoff Simulation of Small Watershed in Loess Hilly Region Using Dynamic Parameter SCS-RF Model. Trans. *Chin. Soc. Agric. Eng.* **2021**, *37*, 195–202.
32. Baghel, S.; Kothari, M.; Tripathi, M.P.; Das, S.; Kumar, A.; Kuriqi, A. Water Conservation Appraisal Using Surface Runoff Estimated by an Integrated SCS-CN and MCDA-AHP Technique. *J. Earth Syst. Sci.* **2023**, *132*, 127. [CrossRef]
33. Tao, D.K.; Zhang, Z.J.; Zhou, W.L.; Wang, Z.Y. Ecological Security Pattern Construction Based on Ecosystem Services Supply-Demand Coordination: A Case Study of Anhui Province. *Planners* **2024**, *40*, 16–24.
34. Weng, W.F.; Li, W.; Xu, S.F.; Chen, Z.R.; Wu, J.; Cao, C.; Zhang, X.N.; Kou, S.W.; Xu, Z.Y.; Xu, H.B.; et al. Geological Relic Resources Types, Characteristics, and Formation in Huangshan City. *East China Geol.* **2020**, *41*, 215–228. [CrossRef]
35. Luan, C.F.; Shi, Z.H.; Zhao, R.J.; Cui, Y.W. Rainwater and Flood Disaster Risk Assessment of Mountainous Small Towns Based on GIS Technology. *People's Yellow River* **2024**, *46*, 56–62+67.
36. Wang, Y.; Li, Z.; Tang, Z.; Zeng, G. A GIS-Based Spatial Multi-Criteria Approach for Flood Risk Assessment in the Dongting Lake Region, Hunan, Central China. *Water Resour. Manag.* **2011**, *25*, 3465–3484. [CrossRef]
37. OECD. *Environmental Indicators: A Preliminary Set*; OECD: Paris, France, 1991.
38. Berge, E. *Air Pollution in Europe 1997*; Jol, A., Kielland, G., Eds.; Office for Official Publications of the European Communities: Brussels, Belgium, 1997.
39. Yu, Y.B.; Zhu, J. Construction and Application of Water Environment Management Performance Evaluation Indicators: A Case Study of Chengdu City. *Sichuan Environ. Sci.* **2019**, *38*, 90–100. [CrossRef]
40. Ness, B.; Anderberg, S.; Olsson, L. Structuring Problems in Sustainability Science: The Multi-Level DPSIR Framework. *Geoforum* **2010**, *41*, 479–488. [CrossRef]
41. Bulut, C.; Arslan, E. Comparison of the Impact of Dimensionality Reduction and Data Splitting on Classification Performance in Credit Risk Assessment. *Artif. Intell. Rev.* **2024**, *57*, 252. [CrossRef]
42. Wang, X.J.; Xia, J.Q.; Li, Q.J.; Zhou, M.R.; Li, B.L. Temporal and Spatial Variation of Flood Disasters and Their Influencing Factors in the Yangtze River Basin. *Water Resour. Prot.* **2023**, *39*, 78–86.
43. Tang, W.; Qi, S.Y.; Yang, X.D.; Li, G.Q. Traffic Flow Data Restoration Based on Random Forest and Nearest Neighbor Interpolation Methods. *Sci. Technol. Eng.* **2024**, *24*, 14056–14065.
44. Zhu, M.L.; Tan, X.L.; Yang, W.L.; Zhang, S.Y.; Zuo, L. Application of Optimized SVM Model in Debris Flow Susceptibility Analysis. *Foreign Electron. Meas. Technol.* **2023**, *42*, 163–170. [CrossRef]
45. Liang, S.; Chen, D.; Li, D.; Qi, Y.; Zhao, Z. Spatial and Temporal Distribution of Geologic Hazards in Shaanxi Province. *Remote Sens.* **2021**, *13*, 4259. [CrossRef]
46. Li, P.L.; Yang, W.; Cai, Z.Y. Flood Risk Zoning in Huide County Based on GIS Technology. *Mod. Agric. Sci. Technol.* **2018**, *2*, 231–233+236.
47. Liu, Y.H.; Han, J.Q.; Xie, M.X.; Shang, T.H.; Zhao, X.L.; Ge, W.Y. Flood Disaster Risk Assessment of the Loess Plateau Based on GIS and AHP Integration. *Res. Soil Water Conserv.* **2023**, *30*, 129–134. [CrossRef]
48. Qiu, Y.; Liu, Y.; Liu, Y.; Chen, Y.Z.; Li, Y. An Interval Two-Stage Stochastic Programming Model for Flood Resources Allocation under Ecological Benefits as a Constraint Combined with Ecological Compensation Concept. *Int. J. Environ. Res. Public Health* **2019**, *16*, 1033. [CrossRef]
49. Den Boer, J.; Dieperink, C.; Mukhtarov, F. Social Learning in Multilevel Flood Risk Governance: Lessons from the Dutch Room for the River Program. *Water* **2019**, *11*, 2032. [CrossRef]
50. Bonasia, R.; Lucatello, S. Linking Flood Susceptibility Mapping and Governance in Mexico for Flood Mitigation: A Participatory Approach Model. *Atmosphere* **2019**, *10*, 424. [CrossRef]

51. An, H.; Zhao, C.W. Study on the Coupling and Coordination Relationship Between Urbanization and Ecological Resilience in Southwest China. *Res. Soil Water Conserv.* **2025**, *32*, 340–352. [CrossRef]
52. Fu, J.H.; Jiang, Z.Y.; Chen, X.; Zhang, W.Z.; Wang, Y.G. Soil and Water Conservation Effect of Biological Fence Terracing Technology on Dry Hillside Farmland. *Tillage Cultiv.* **2000**, *6*, 1–10.